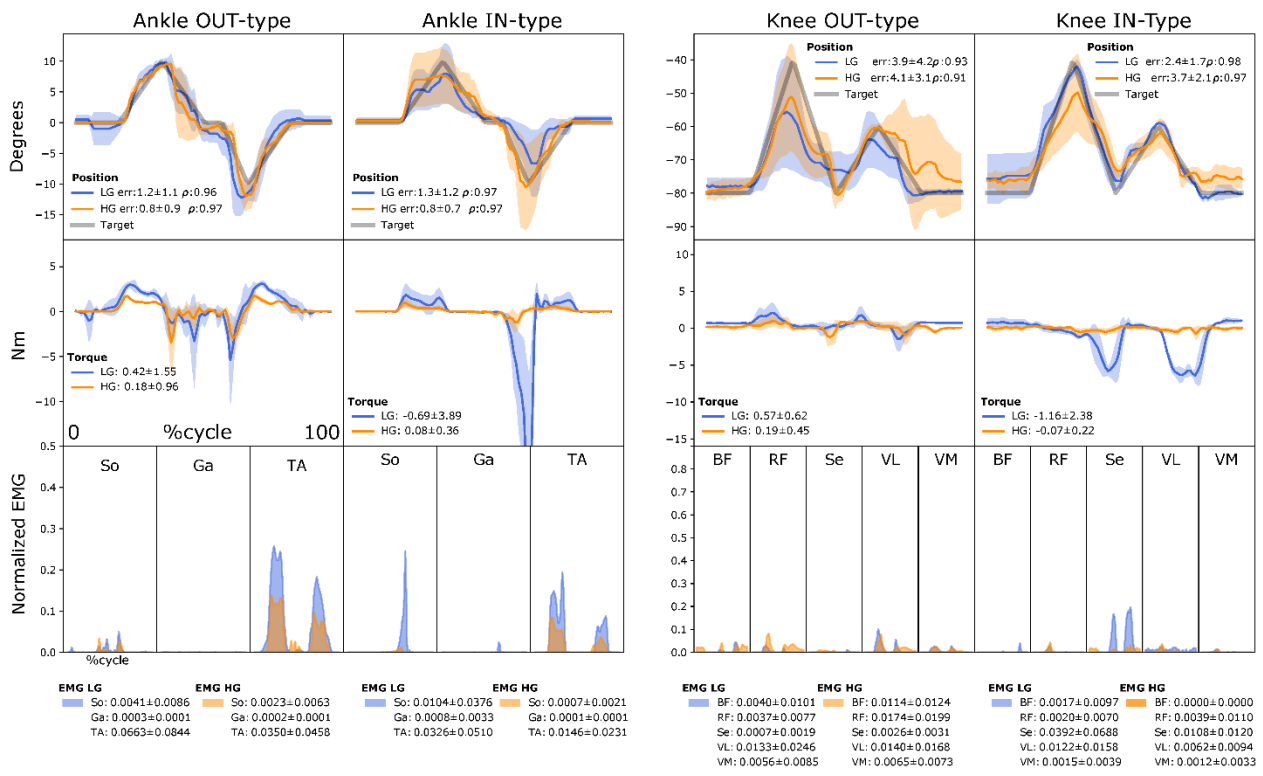


22

23 **Supplementary figure S1. Tracking task performance during single-DOF tests for healthy subject 3.**

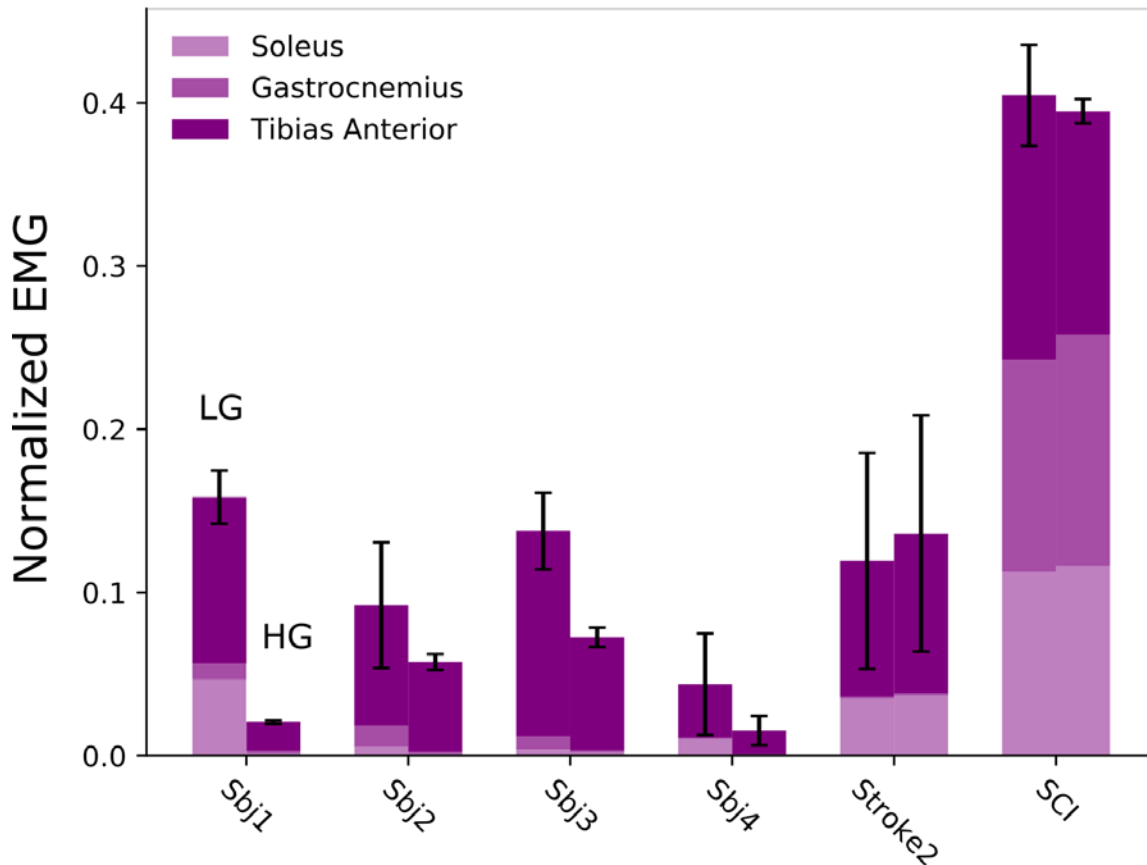
24 Exoskeleton joint angular position, electromyography (EMG) data as well as model-based estimates of joint
 25 moments (torque) are reported during single degree of freedom (DOF) tasks. Data are reported as averaged
 26 across all tracking trials. They are reported for the low-gain (LG) and high-gain (HG) exoskeletons assistance
 27 levels and as a function of percent cycle, i.e. where 0% and 100% respectively represents the beginning and
 28 the end of the tracking trajectory (Target). Results are relative to tests outside and inside of the exoskeleton
 29 respectively, i.e. OUT-type and IN-type. Results are reported both for the individual control of the exoskeleton
 30 ankle plantar-dorsiflexion DOF and for that of the exoskeleton knee flexion-extension DOF. EMGs are relative
 31 to muscles including: biceps femoris (BF), rectus femoris (RF), semimembranosus (S), vastus lateralis (VL)
 32 and vastus medialis (VM), soleus (So), gastrocnemius medialis (Ga) and tibia anterior (TA), i.e. Table 2.
 33 Average ± standard deviation of EMG linear envelopes are reported at the bottom of the graph.

34



35
 36 **Supplementary figure S2. Tracking task performance during single-DOF tests for healthy subject 4.**
 37 Exoskeleton joint angular position, electromyography (EMG) data as well as model-based estimates of joint
 38 moments (torque) are reported during single degree of freedom (DOF) tasks. Data are reported as averaged
 39 across all tracking trials. They are reported for the low-gain (LG) and high-gain (HG) exoskeletons assistance
 40 levels and as a function of percent cycle, i.e. where 0% and 100% respectively represents the beginning and
 41 the end of the tracking trajectory (target). Results are relative to tests outside and inside of the exoskeleton, i.e.
 42 OUT-type and IN-type respectively. Results are reported both for the individual control of the exoskeleton
 43 ankle plantar-dorsiflexion DOF and for that of the exoskeleton knee flexion-extension DOF. EMGs are relative
 44 to muscles including: biceps femoris (BF), rectus femoris (RF), semimembranosus (S), vastus lateralis (VL)
 45 and vastus medialis (VM), soleus (So), gastrocnemius medialis (Ga) and tibias anterior (TA), i.e. Table 2.
 46 Average ± standard deviation of EMG linear envelopes are reported at the bottom of the graph.

EMG Reduction Ankle IN-type



47

48

49

50

51

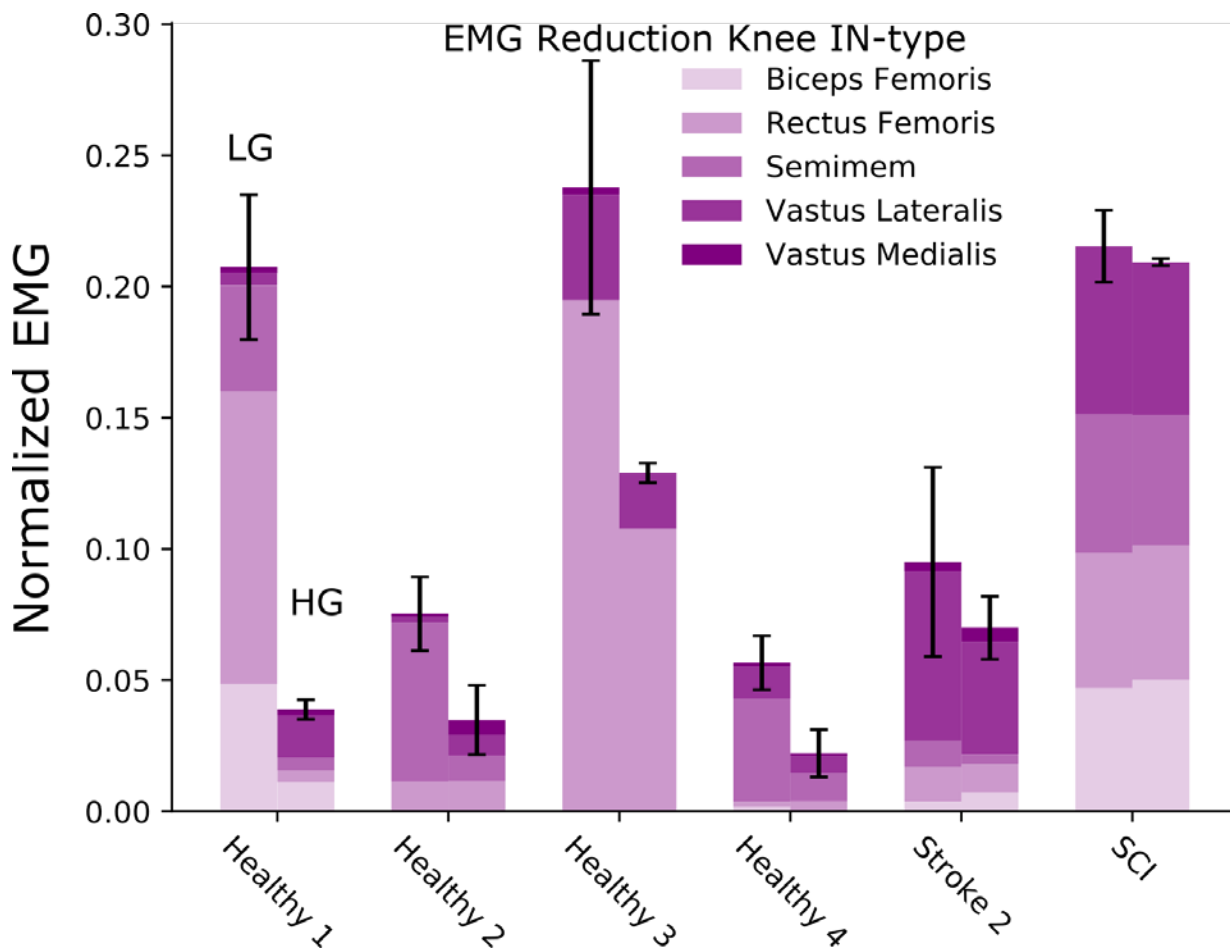
52

53

54

55

Supplementary figure S3. EMG amplitude modulation between exoskeleton low- and high-assistance levels during single ankle plantar-dorsi flexion, IN-type experiments. Electromyography (EMG) amplitude is consistently reduced when transitioning from low-gain (LG, left-hand vertical bar) to high-gain (HG, right-hand vertical bar) exoskeleton support levels. Experiments were performed while wearing the robotic exoskeleton, i.e. IN-type tests. For each subject (Healthy 1-4) as well as for stroke patient 2 (Stroke) and the spinal cord injury (SCI) patient (Table 1) the vertical bars report mean normalised EMG amplitude stacked vertically for each muscles along with standard deviation (i.e. see black vertical lines).



56

57

58

59

60

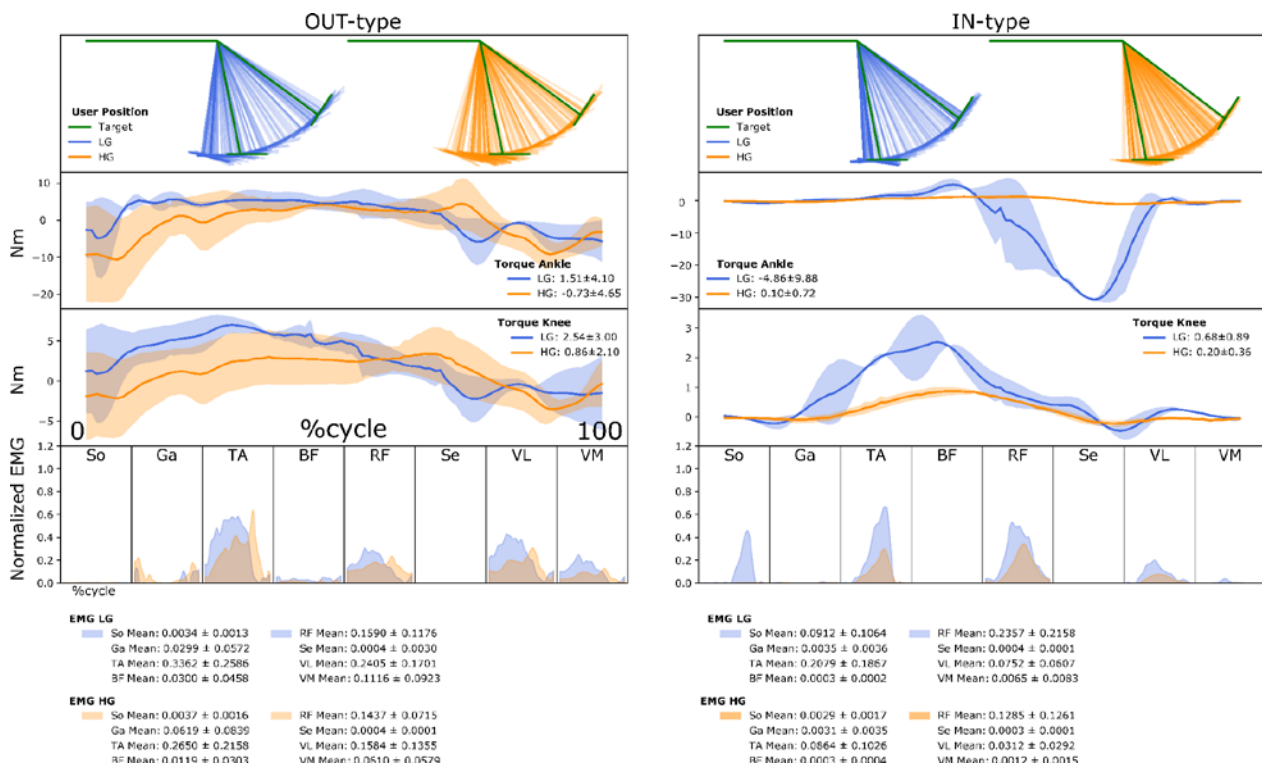
61

62

63

64

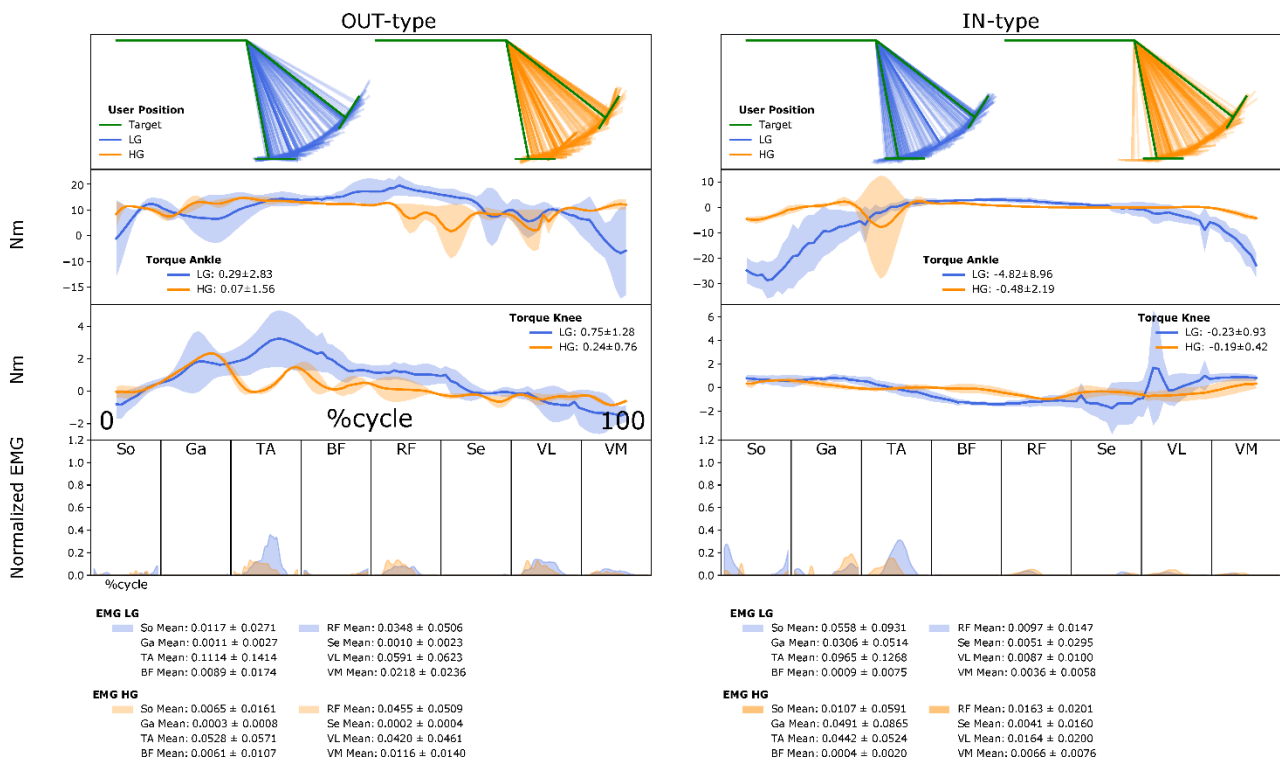
Supplementary figure S4. EMG amplitude modulation between exoskeleton low- and high-assistance levels during single knee flexion-extension, IN-type experiments. Electromyography (EMG) amplitude is consistently reduced when transitioning from low-gain (LG, left-hand vertical bar) to high-gain (HG, right-hand vertical bar) exoskeleton support levels. Experiments were performed while wearing the robotic exoskeleton, i.e. IN-type tests. For each subject (Healthy 1-4) as well as for stroke patient 2 (Stroke) and the spinal cord injury (SCI) patient (Table 1) the vertical bars report mean normalised EMG amplitude stacked vertically for each muscles along with standard deviation (i.e. see black vertical lines).



65

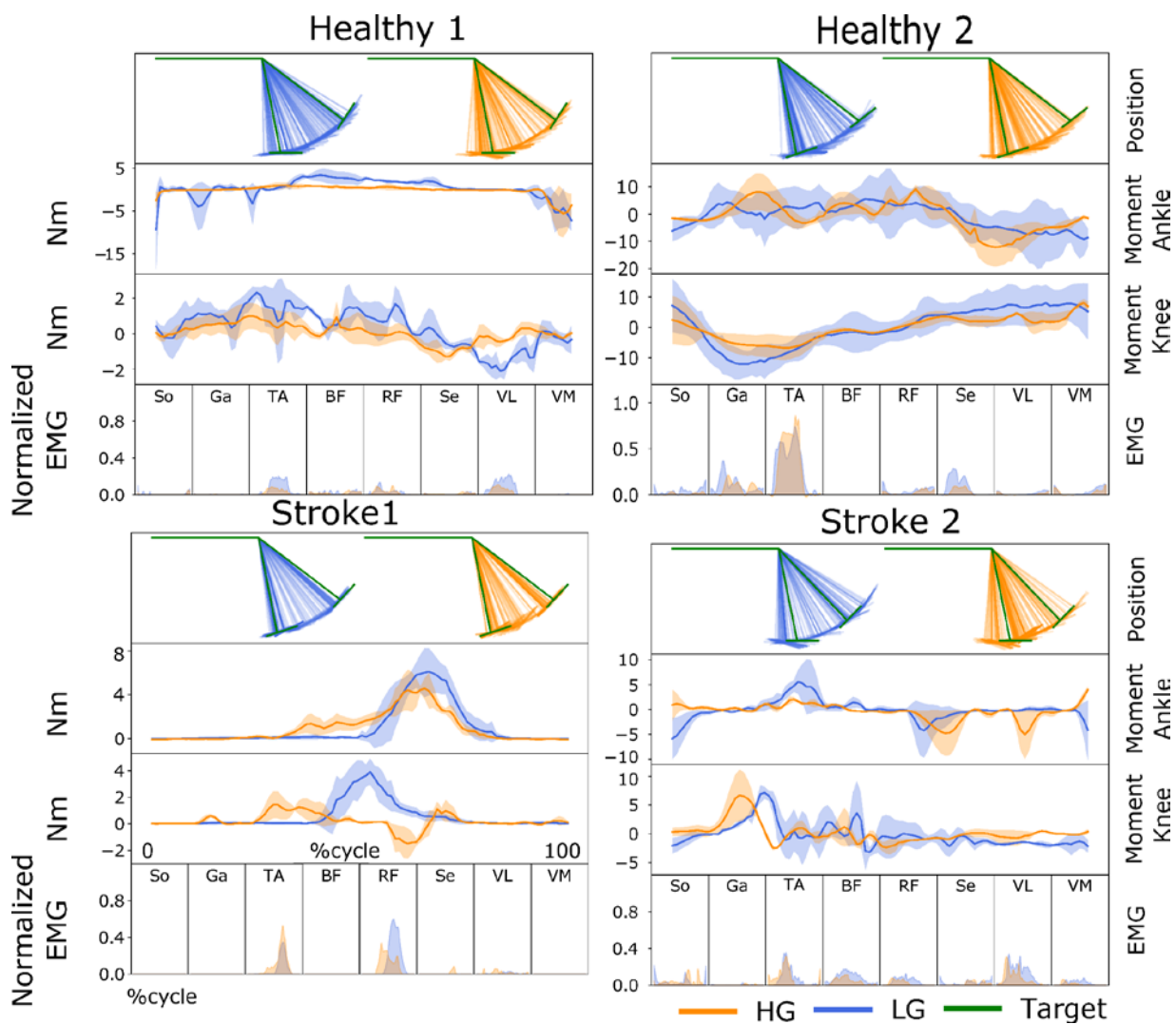
66 **Supplementary figure S5: Tracking task performance during multi-DOF, OUT- and IN-type tests for**
 67 **healthy subject 3.** Exoskeleton knee and ankle joint angular positions are reported by means of a stick-figure.
 68 The green figure represents the target multi-joint position to be tracked. The blue and orange stick-figures
 69 respectively represent the subject's voluntary controlled exoskeleton trajectory obtained using a low-gain (LG)
 70 and high-gain (HG) assistance levels. Model-based estimates of joint moments (torque) are reported both about
 71 the knee flexion-extension and ankle plantar-dorsi flexion degree of freedom (DOFs). Data are reported as
 72 averaged across all tracking trials. They are reported as a function of percent cycle, i.e. where 0% and 100%
 73 respectively represents the beginning and the end of the tracking trajectory (target). Recorded
 74 electromyography (EMGs) signals are relative to muscles including: biceps femoris (BF), rectus femoris (RF),
 75 semimembranosus (S), vastus lateralis (VL) and vastus medialis (VM), soleus (So), gastrocnemius medialis
 76 (Ga) and tibias anterior (TA), i.e. Table 2. Average \pm standard deviation of EMG linear envelopes are reported
 77 at the bottom of the graph.

78



79

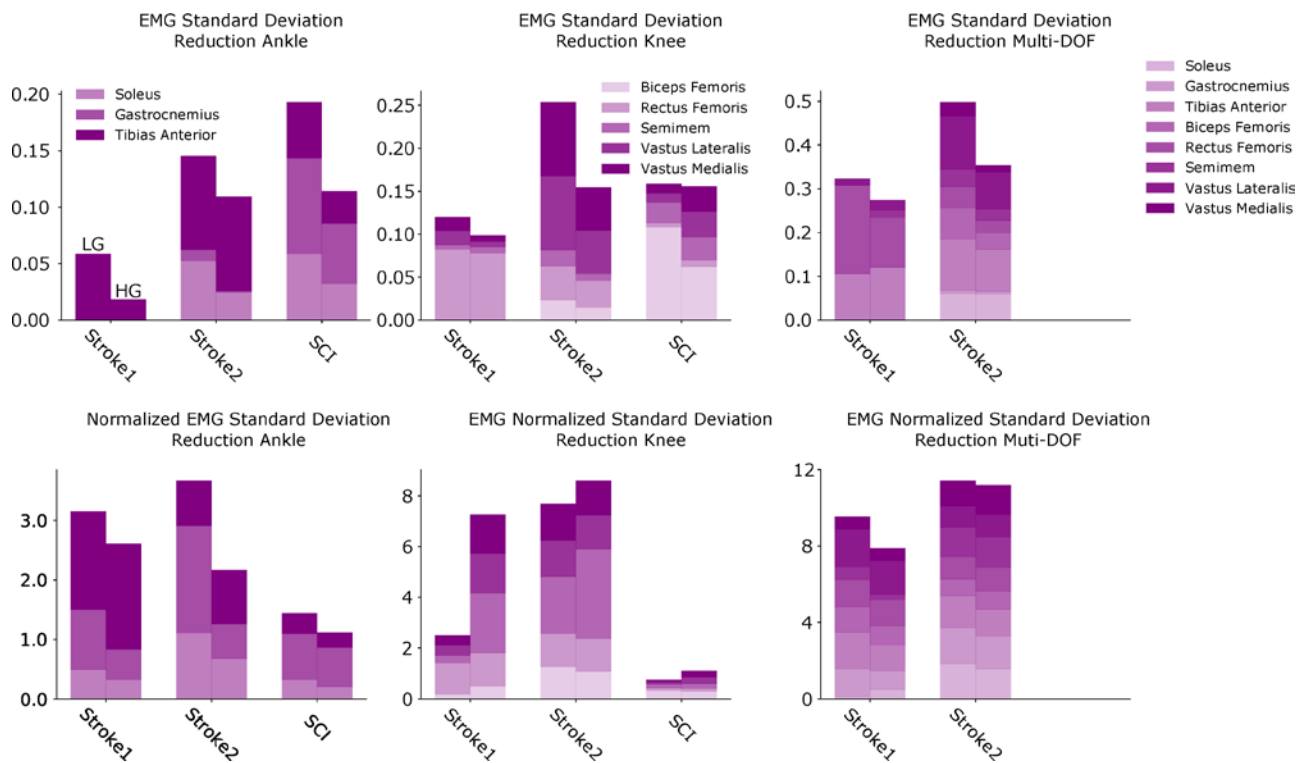
80 **Supplementary figure S6: Tracking task performance during multi-DOF, OUT- and IN-type tests for**
 81 **healthy subject 4.** Exoskeleton knee and ankle joint angular positions are reported by means of a stick-figure.
 82 The green figure represents the target multi-joint position to be tracked. The blue and orange stick-figures
 83 respectively represent the subject's voluntary controlled exoskeleton trajectory obtained using a low-gain (LG)
 84 and high-gain (HG) assistance levels. Model-based estimates of joint moments (torque) are reported both about
 85 the knee flexion-extension and ankle plantar-dorsi flexion degree of freedom (DOFs). Data are reported as
 86 averaged across all tracking trials. They are reported as a function of percent cycle, i.e. where 0% and 100%
 87 respectively represents the beginning and the end of the tracking trajectory (target). Recorded
 88 electromyography (EMGs) signals are relative to muscles including: biceps femoris (BF), rectus femoris (RF),
 89 semimembranosus (S), vastus lateralis (VL) and vastus medialis (VM), soleus (So), gastrocnemius medialis
 90 (Ga) and tibias anterior (TA), i.e. Table 2. Average \pm standard deviation of EMG linear envelopes are reported
 91 at the bottom of the graph.



92

93 **Supplementary figure S7. Tracking task performance during multi-DOF, OUT-type tests.** Exoskeleton
 94 knee and ankle joint angular positions are reported by means of a stick-figure. The green figure represents the
 95 target multi-joint position to be tracked. The blue and orange stick-figures respectively represent the subject's
 96 voluntarily controlled exoskeleton trajectory obtained using a low-gain (LG) and high-gain (HG) assistance
 97 levels. Model-based estimates of joint moments are reported both about the knee flexion-extension and ankle
 98 plantar-dorsi flexion degree of freedom (DOFs). Data are reported as averaged across all tracking trials. They
 99 are reported as a function of percent cycle, i.e. where 0% and 100% respectively represents the beginning and
 100 the end of the tracking trajectory (Target). Results are relative to tests inside of the exoskeleton, i.e. OUT-type.
 101 Data are reported for two representative healthy subjects (Healthy 1-2) and two stroke patients (Stroke 1-2),
 102 i.e. Table 1. Recorded electromyography (EMGs) signals are relative to muscles including: biceps femoris
 103 (BF), rectus femoris (RF), semimembranosus (S), vastus lateralis (VL) and vastus medialis (VM), soleus (So),
 104 gastrocnemius medialis (Ga) and tibialis anterior (TA), i.e. Table 2.

105



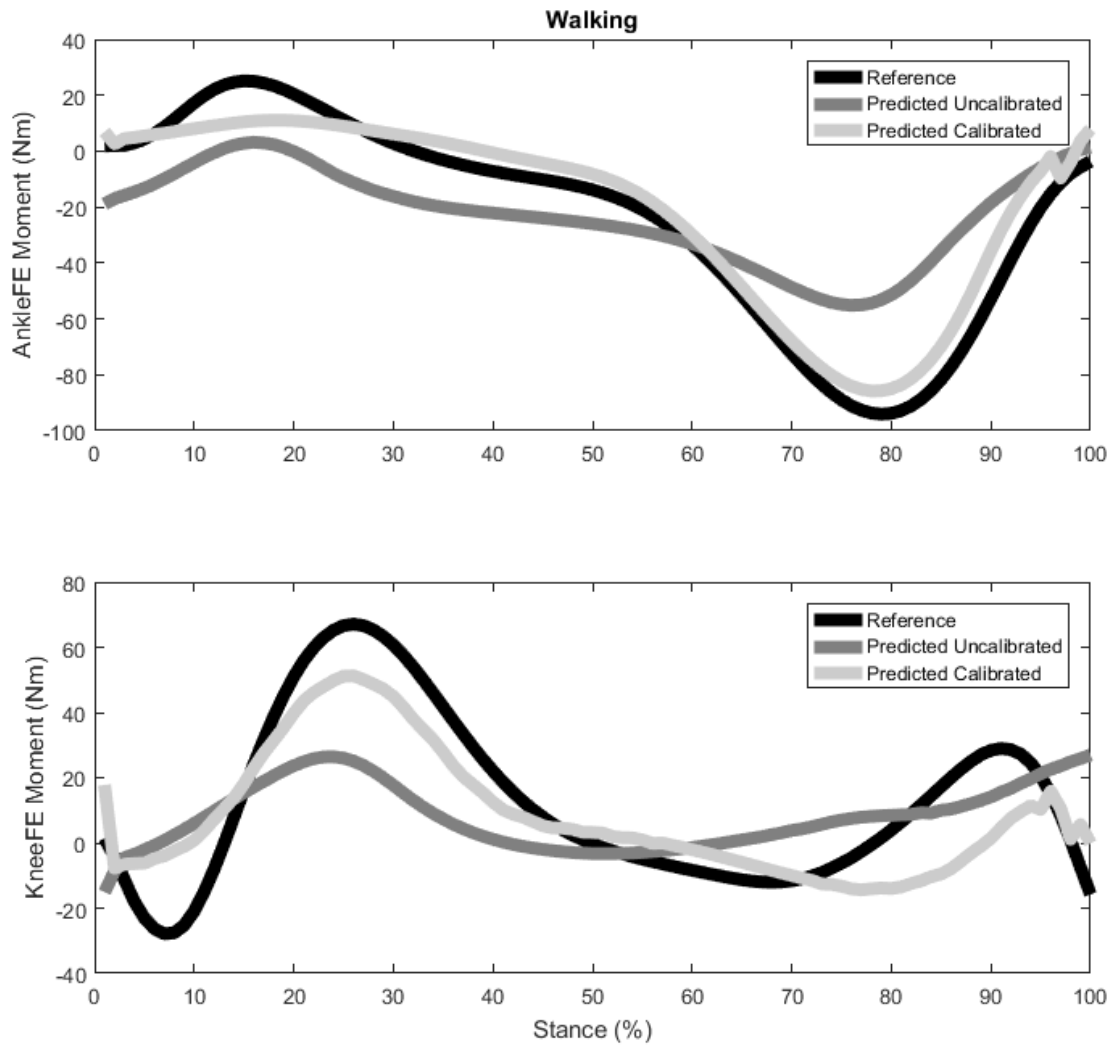
106

107 **Supplementary figure S8. Standard deviation of the mean EMG amplitude during single-DOF and**
 108 **multi-DOF, OUT-type tests.** Histograms report non-normalized standard deviation (top-row) and normalized
 109 standard deviation (bottom-row, Eq. 3) extracted from electromyography (EMG) data across of all trials
 110 performed during single-ankle control tasks, single-knee control tasks as well as simultaneous ankle-knee
 111 control tasks. Histograms are reported relative to low-gain (LG) and high-gain (HG) assistance levels. Data
 112 are relative to stroke patient 2 and to the incomplete spinal cord injury patient (SCI), Table 1.

113

114

115



116

117 **Supplementary figure S9. Predicted moment for the Ankle plantar-dorsiflexion and the Knee flexion-**
 118 **extension using an uncalibrated model.** Average of 5 subjects for a locomotion task (fast walking), with in
 119 grey line the predicted moment using a uncalibrated model, in light grey the predicted moment using a
 120 calibrated model and in black line the experimental moment from inverse dynamics using the OpenSim
 121 Software. Data taken from (1).

122

123

<i>Sbjs</i>	Ankle OUT-type N.m (mean± std)		Knee OUT-type N.m (mean± std)		Multi-DOF OUT-type N.m (mean± std)				Ankle IN-type N.m (mean± std)		Knee IN-type N.m (mean± std)		Multi-DOF IN-type N.m (mean± std)			
					Knee		Ankle						Knee		Ankle	
	HG	LG	HG	LG	HG	LG	HG	LG	HG	LG	HG	LG	HG	LG	HG	LG
<i>Sbj1</i>	0.81	1.24	0.50	1.31	0.71	1.34	1.42	2.97	0.44	10.6	0.69	5.57	1.69	6.26	5.40	13.7
	±	±	±	±	±	±	±	±	±	±	±	±	±	±	±	±
<i>Sbj2</i>	0.24	0.87	0.09	0.39	0.11	0.05	0.88	0.20	0.03	1.61	0.03	0.87	0.40	0.33	4.81	2.48
	±	±	±	±	±	±	±	±	±	±	±	±	±	±	±	±
<i>Sbj3</i>	1.83	3.79	1.22	3.5	4.50	8.33	6.34	8.18	1.25	3.28	1.72	3.97	5.17	7.22	18.3	14.0
	±	±	±	±	±	±	±	±	±	±	±	±	±	±	±	±
<i>Sbj4</i>	0.24	0.73	0.33	2.1	0.98	0.94	2.09	1.55	0.24	0.79	0.51	1.26	1.72	1.57	6.61	4.95
	±	±	±	±	±	±	±	±	±	±	±	±	±	±	±	±
<i>Stroke 1</i>	1.11	2.18	1.11	2.96	3.72	4.57	6.80	5.55	0.35	2.37	0.20	0.62	0.41	1.19	0.77	11.8
	±	±	±	±	±	±	±	±	±	±	±	±	±	±	±	±
<i>Stroke 2</i>	0.40	1.07	0.56	0.16	1.15	0.38	2.81	1.19	0.05	1.73	0.01	0.10	0.05	0.12	0.09	0.02
	±	±	±	±	±	±	±	±	±	±	±	±	±	±	±	±
<i>SCI</i>	1.18	2.03	0.73	1.03	0.85	1.69	2.17	3.87	0.41	4.01	0.39	2.83	0.57	1.25	3.31	10.9
	±	±	±	±	±	±	±	±	±	±	±	±	±	±	±	±
<i>Stroke 1</i>	0.20	0.38	0.06	0.17	0.03	0.44	0.13	1.29	0.23	2.83	0.03	0.26	0.04	0.54	3.66	2.15
	±	±	±	±	±	±	±	±	±	±	±	±	±	±	±	±
<i>Stroke 2</i>	0.82	2.85	0.38	0.69	0.73	1.25	1.72	2.17	N/A	N/A	N/A	N/A	N/A	N/A	N/A	N/A
	±	±	±	±	±	±	±	±	±	±	±	±	±	±	±	±
<i>SCI</i>	0.62	1.67	0.15	0.18	0.14	0.09	0.08	0.46	N/A	N/A	N/A	N/A	N/A	N/A	N/A	N/A
	±	±	±	±	±	±	±	±	±	±	±	±	±	±	±	±
<i>Stroke 2</i>	1.51	2.98	0.89	2.15	2.10	2.80	2.20	2.50	1.12	1.62	1.31	2.10	3.61	7.21	3.16	6.86
	±	±	±	±	±	±	±	±	±	±	±	±	±	±	±	±
<i>SCI</i>	1.02	0.75	0.44	0.21	0.70	0.34	0.25	1.11	0.57	0.96	0.07	1.00	0.72	1.16	0.98	0.60
	±	±	±	±	±	±	±	±	±	±	±	±	±	±	±	±
<i>SCI</i>	3.82	6.65	3.07	7.10	N/A	N/A	N/A	N/A	4.29	7.14	1.49	1.62	1.15	1.63	3.58	4.88
	±	±	±	±	N/A	N/A	N/A	N/A	±	±	±	±	±	±	±	±
<i>SCI</i>	1.37	2.28	0.77	0.77	N/A	N/A	N/A	N/A	0.24	0.35	0.08	0.47	0.01	0.00	0.17	0.28
	±	±	±	±	N/A	N/A	N/A	N/A	±	±	±	±	±	±	±	±

126 **Supplementary Table S1: Joint moment modulation across assistance levels.** Root mean squared sum of
127 joint moments averaged across all trials for each subject and condition, i.e. see Figs 2-3, 5-6. Data are reported
128 both relative to the low-gain (LG) and high-gain (HG) exoskeleton assistance levels.

	Ankle OUT-type		Knee OUT-type		Multi-DOF OUT-type				Ankle IN-type		Knee IN-type		Multi-DOF IN-type			
	HG	LG	HG	LG	Knee		Ankle		HG	LG	HG	LG	Knee		Ankle	
					HG	LG	HG	LG					HG	LG	HG	LG
Stroke 1	5.0	2.0	20	10	5.0	2.5	20	10	N/A	N/A	N/A	N/A	N/A	N/A	N/A	N/A
Stroke 2	10	5.0	10	5.0	10	5.0	10	5.0	6.0	3.0	7.0	3.0	6.0	3.0	5.0	3.0
SCI	2.0	1.0	2.0	1.0	N/A	N/A	N/A	N/A	2.0	1.0	3.0	6.0	2.0	1.0	6.0	3.0

131 **Supplementary Table S2: Gain used for the assistance for the patients.** This gain were used during the
132 experiments were they determined the assistance given by the exoskeleton. This gain were sectioned to give
133 comfortable assistance and were determined experimentally.

134

135

- 136 1. Sartori M, Maculan M, Pizzolato C, Reggiani M, Farina D, Claudio P, et al. Modeling and simulating
137 the neuromuscular mechanisms regulating ankle and knee joint stiffness during human locomotion. *J*
138 *Neurophysiol.* 2015;114(4):2509–27.

139